

### Charge-transfer transitions of Fe ions in InP

K. Thonke

*Abteilung Halbleiterphysik, Universität Ulm, D-7900 Ulm, Germany*

K. Pressel

*4. Physikalisches Institut, Universität Stuttgart, D-7000 Stuttgart 80, Germany*

(Received 25 July 1991)

We study, in detail, optical transitions of Fe ions in InP. Spectra recorded at different sample temperatures allow reliable assignments of absorption peaks to 3*d* internal transitions of Fe<sup>2+</sup>. Charge-transfer processes from Fe<sup>3+</sup> to Fe<sup>2+</sup> plus a bound hole give rise to multiple absorption bands in the energy range from 6100 to 10000 cm<sup>-1</sup>. For both the Fe<sup>2+</sup> ion and the bound hole, a series of excited states are observed. In the ground state of the bound hole, a strong interaction with the *d*-shell electrons of the Fe<sup>2+</sup> ion diminishes the spin-orbit coupling to 72% of its original value. By comparison with shallow effective-mass-like acceptor series, the hole binding energy of the Fe<sup>2+</sup> ion is derived. This allows an exact location of the Fe<sup>2+</sup> levels in the band gap to be determined.

#### I. INTRODUCTION

Fe atoms introduced into InP replace In atoms and act as deep acceptors. In the charge state 2+ (3*d*<sup>6</sup>, *L*=2, *S*=2), crystal field and spin-orbit interaction result in a splitting of states as depicted in the left-hand part of Fig. 1.<sup>1</sup> The splitting of the upper <sup>5</sup>*T*<sub>2</sub> manifold is of the order of 5 times the free ion spin-orbit coupling parameter λ. The degeneracy of the lower <sup>5</sup>*E* manifold is only lifted via interaction with the <sup>5</sup>*T*<sub>2</sub> upper state. The <sup>5</sup>*E* states are split with energies of ≅ λ<sup>2</sup>/*Dq*. Mixing of these states with excited states of odd parity, mediated by the odd part *U*<sup>3</sup> of the crystal field, makes optical transitions allowed.<sup>2</sup> In InP the existence of the Fe<sup>3+</sup> state is verified by electron spin resonance, and the Fe<sup>2+</sup> state is detected in optical measurements. In the charge state Fe<sup>2+</sup> (3*d*<sup>6</sup>) optical measurements show four zero-phonon (ZP) lines between 2800 and 2845 cm<sup>-1</sup>, which were observed by Koschel, Kaufman, and Bishop<sup>3</sup> in photoluminescence (PL) and absorption experiments. These lines were ascribed to internal transitions within the 3*d* shell.

The associated phonon sidebands were studied in detail before.<sup>4,5</sup> For the ZP lines, different half-widths are found, which vary with temperature. We analyze this temperature dependence in the present contribution. In the energy range some 100 cm<sup>-1</sup> above the ZP lines, internal *d*-shell transitions to excited <sup>5</sup>*T*<sub>2</sub> levels were detected.<sup>5</sup>

Charge-transfer (CT) processes from Fe<sup>3+</sup> to Fe<sup>2+</sup> were observed by calorimetric absorption spectroscopy (CAS),<sup>6</sup> and later by conventional infrared absorption spectroscopy,<sup>7</sup> and in Fourier transform infrared (FTIR) absorption studies.<sup>8</sup> We present here a much more detailed study where, due to better resolution and improved signal-to-noise ratio, several additional features are revealed. We find a series of excited states for a hole bound to Fe<sup>2+</sup>, and a strong interaction of this bound hole in its ground state with the *d*-shell Fe electrons. Some of the previously found features have to be reassigned.

All the absorption spectra were recorded with a BOMEM DA3.01 Fourier-transform spectrometer, which offers a maximum unapodized resolution of 0.01 cm<sup>-1</sup>. In the energy range around 3000 cm<sup>-1</sup> an InSb detector was used, whereas for the range of 6000 to 10000 cm<sup>-1</sup> an In-Ga-As diode was mounted to the FTIR spectrometer.

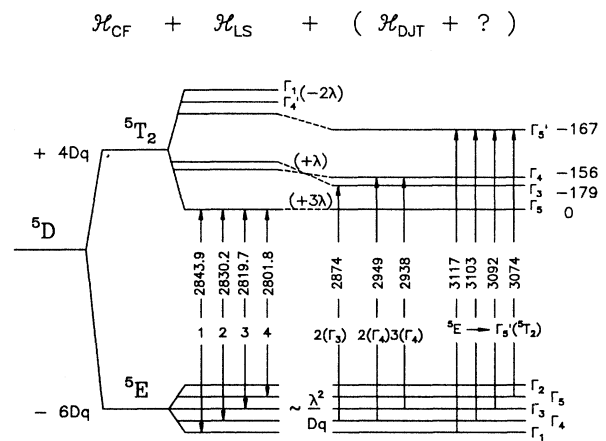


FIG. 1. Level scheme for the InP:Fe<sup>2+</sup> 3*d* internal transitions. The <sup>5</sup>*D* state is split by crystal-field and spin-orbit interactions. The position of the <sup>5</sup>*T*<sub>2</sub> substates depends, in first-order perturbation theory, linearly on the spin-orbit coupling λ, whereas the <sup>5</sup>*E* substates are split proportional to λ<sup>2</sup>/*Dq* in second-order perturbation theory. Arrows indicate the optical transitions observed in PL or absorption; the included numbers are the respective transition energies in cm<sup>-1</sup>. The parameters *Dq* and λ were fitted to the energies of the four main PL transitions 1–4. Relative to the positions of the excited <sup>5</sup>*T*<sub>2</sub> states calculated from these numbers, lowerings are found experimentally, which are quoted on the right-hand side of the <sup>5</sup>*T*<sub>2</sub> states. The lowerings must be due to a dynamical Jahn-Teller effect (*H*<sub>DJT</sub>), covalency effects and mixing with higher states.

## II. INTERNAL 3d TRANSITIONS AT Fe<sup>2+</sup> IN InP

Figure 2 presents a series of absorption spectra of the Fe<sup>2+</sup> 3d internal transitions in the energy range between 2790 and 3200 cm<sup>-1</sup>. The low-temperature spectrum at 2.1 K only shows the zero-phonon line 1 (ZP1) at 2843.9 cm<sup>-1</sup> out of the four allowed transitions of the <sup>5</sup>E ground state to the  $\Gamma_5(^5T_2)$  excited state. With rising temperature ZP2 and the other hot lines appear according to thermal population of the initial <sup>5</sup>E sublevels (compare with Fig. 1). Besides the four characteristic ZP lines at 2800–2845 cm<sup>-1</sup>, the most prominent feature in the absorption phonon sideband of the Fe<sup>2+</sup> ion is a Fe-defect-specific (gap) mode GM1\* with an energy of 292 cm<sup>-1</sup>,<sup>5</sup> which will be important in analyzing the CT transitions in the following section.

In most of the samples, line ZP1 has Gaussian line shape in the absorption spectrum at ~2.1 K. Its full width at half maximum (FWHM) can be less than 0.02 cm<sup>-1</sup> in appropriate samples.<sup>5</sup> The half-width is obviously determined by residual microscopic random strain in the majority of samples (external strain was avoided by careful mounting of the samples). Temperature increase to ~7 K results in a broader FWHM of ZP1 and ZP2, and changes their line shape from Gaussian to Lorentzian. Phonons absorbed from the thermal background can eject electrons into the close lying excited states thus reducing the effective lifetime of either the initial or final state of the transition.

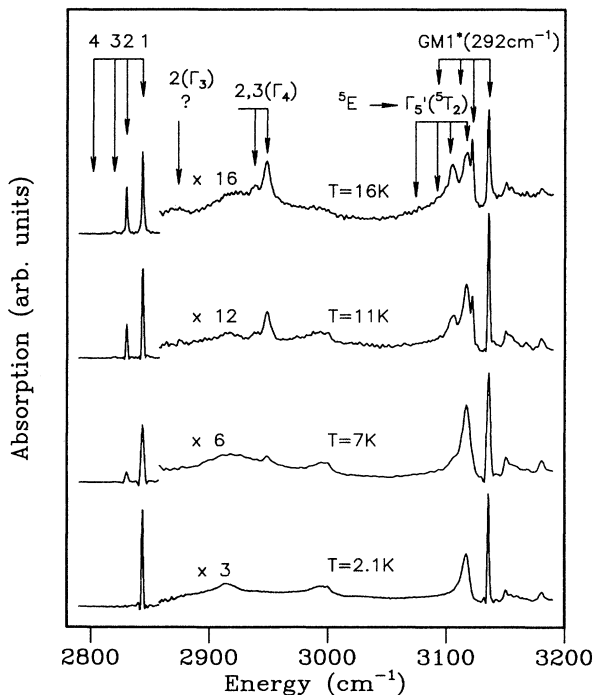


FIG. 2. Absorption spectra of the 3d internal transitions of InP:Fe<sup>2+</sup> recorded at different sample temperatures. Besides the four zero phonon lines 1–4 and their phonon replica GM1\* we observe several other electronic transitions to excited <sup>5</sup>T<sub>2</sub> states (compare Fig. 1). The spectra were normalized such that the area under ZP1 is constant.

In the temperature range where the line shape is Lorentzian, the FWHM is determined by the effective lifetime of both the initial or final state, with  $\Gamma = \hbar/\tau$ , where  $\Gamma$  is the linewidth and  $\tau$  is the effective lifetime. For  $\tau$  holds

$$1/\tau = 1/\tau_i + 1/\tau_f, \quad (1)$$

where  $\tau_i$  and  $\tau_f$  stand for the lifetimes of the initial and final state of the transition, respectively. The time constants  $\tau_i$  and  $\tau_f$ , in turn, are affected by radiative processes and nonradiative processes, like thermal excitation of carriers to excited states. In such cases,  $\tau_i$  (or  $\tau_f$ ) is temperature dependent with

$$1/\tau_i = 1/\tau_{i,r} + \sum_k 1/\tau_{i,k} e^{-\Delta E_{ik}/k_B T}. \quad (2)$$

The first term,  $\tau_{i,r}$ , stands for radiative recombinations, whereas the sum adds up processes of thermal ejection of carriers to excited states. This means for the half-width a temperature dependence like

$$\Delta E_{\text{FWHM}}(T) = F_0 + \sum F_k \exp(-E_k/k_B T) \quad (3)$$

when other broadening mechanisms like residual strain are neglected. Figure 3 shows in an Arrhenius plot for three different samples the change of the FWHM of lines ZP1 and ZP2, which for  $T > 6$  K have Lorentzian shape.

The FWHM of ZP1 and ZP2 differs slightly below 10

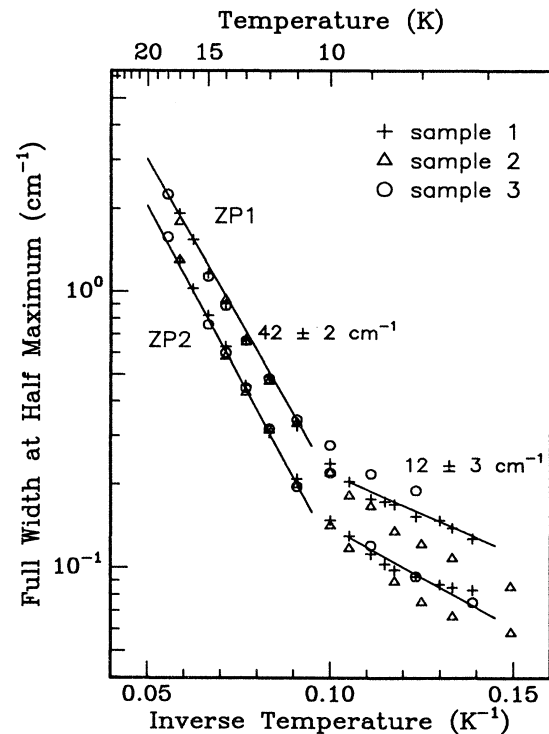


FIG. 3. Temperature dependence of the half-width of zero phonon lines 1 and 2 in absorption. The half-width is determined by lifetime effects. For both transitions the lifetime is reduced by thermally activated processes with  $\approx 12$  and  $42$  cm<sup>-1</sup> activation energy.

K in all our samples, the linewidth of ZP2 being always less than that of ZP1. As for both ZP1 and ZP2, the underlying transitions have the  $\Gamma_5(^5T_2)$  as final state in absorption (Fig. 1). Therefore, the difference in the absorption linewidth must have its origin in the initial states  $\Gamma_1(^5E)$  and  $\Gamma_4(^5E)$ , respectively. Thus for the  $\Gamma_1(^5E)$  a shorter lifetime must be concluded than for the  $\Gamma_4(^5E)$ . Two regions can be distinguished: between 6 and 10 K the linewidth increases due to a thermally activated process with 10–15-cm<sup>-1</sup> activation energy. We ascribe this activation energy for both ZP1 and ZP2 to an excitation within the  $^5E$  ladder of states, which has a spacing of 13.7 and 10.4 cm<sup>-1</sup> (Ref. 5) for the three lowest states.

Above 10 K, a second parallel process with ~40–45-cm<sup>-1</sup> activation energy becomes efficient. This further decrease of lifetime can be due in part to excitation into higher states within the  $^5E$  manifold, but since the curves for both ZP1 and ZP2 are parallel over a certain range, we believe the underlying process to occur at the  $\Gamma_5(^5T_2)$  final state, which is common for both lines.<sup>9</sup>

Temperature-dependent absorption spectra (Fig. 2) allow us to detect several transitions from the  $^5E$  ground state to excited sublevels of the  $^5T_2$  state. All these transitions are summarized in the right-hand part of Fig. 1.

At 273 cm<sup>-1</sup> above the zero-phonon lines ZP1 and ZP2 we observe two relatively broad lines, the line at lower energy coming up stronger with rising temperature. The relative intensities closely follow the ZP1 and ZP2 lines and show a spacing identical to these lines. Since we find no corresponding lines with equal energetic shift on the Stokes side in emission, we ascribe these lines to electronic transitions.<sup>5,8</sup> Selection rules allow for the lowest  $\Gamma_1(^5E)$  state only electronic dipole transitions to states of  $\Gamma_5$  nature. Therefore these two lines must be transitions from  $\Gamma_1(^5E)$  to  $\Gamma_5(^5T_2)$ , and from  $\Gamma_4(^5E)$  to  $\Gamma_5(^5T_2)$  (see right-hand part of Fig. 1). With rising temperature, contributions of transitions from the higher  $^5E$  states  $\Gamma_3(^5E)$  and  $\Gamma_5(^5E)$  to the  $\Gamma_5(^5T_2)$  also appear, weakly showing up with the same energetic spacing pattern as the four ZP lines. This pattern is indicated by the set of arrows denoted by  $^5E \rightarrow \Gamma_5(^5T_2)$  in Fig. 2.

We ascribe the relatively large FWHM of these lines to a lifetime broadening affecting the upper state of the transitions. From the FWHM of ~7 cm<sup>-1</sup> we conclude that the electron in the excited state must relax into the  $\Gamma_5(^5T_2)$  lowest  $^5T_2$  substate within some  $4 \times 10^{-13}$  sec, a value realistic for thermalization mediated by electron-phonon coupling. The value of 273 cm<sup>-1</sup> obtained for the spacing of the  $\Gamma_5(^5T_2)$  state from  $\Gamma_5(^5T_2)$  which we find here for InP:Fe is comparable to the values of 303 cm<sup>-1</sup> for GaP:Fe,<sup>10</sup> and 249 cm<sup>-1</sup> for GaAs:Fe (Ref. 11) for the respective splittings.

When the sample temperature is increased above 6 K, a hot line absorption shows up at 2948.6 cm<sup>-1</sup>. We considered this line earlier as the anti-Stokes line of a resonant mode named RM1 observed in PL.<sup>8</sup> But new absorption measurements on thicker samples, recorded at sample temperatures down to 2.1 K, clearly identify this line as a hot line, i.e., a transition starting on an excited ground-state level not occupied at low temperature. The

2.1-K spectrum does not show this peak at 2948.6 cm<sup>-1</sup>, but at about 6 K this peak appears and increases with rising temperature. Adjacent to this hot line (10.7 cm<sup>-1</sup> lower in energy at 2937.9 cm<sup>-1</sup>) a further hot line comes in around 11 K. This is precisely the spacing between the second and third  $^5E$  states  $\Gamma_4(^5E)$  and  $\Gamma_3(^5E)$ , and can be clearly distinguished from the 13.7-cm<sup>-1</sup> spacing between the lowest  $^5E$  states  $\Gamma_1(^5E)$  and  $\Gamma_4(^5E)$ .

Group theory allows electric dipole transitions between  $\Gamma_4 \leftrightarrow \Gamma_4$  and  $\Gamma_4 \leftrightarrow \Gamma_3$ , but not between  $\Gamma_3 \leftrightarrow \Gamma_3$ . Therefore, the hot lines at  $\approx 2950$  cm<sup>-1</sup> must be ending on the  $\Gamma_4(^5T_2)$  level. This locates the  $\Gamma_4(^5T_2)$  substate 118.5 cm<sup>-1</sup> above the lowest  $\Gamma_5(^5T_2)$  level. The assignment of the series to internal  $3d$  transition will also be confirmed in the following discussion of spectra in the 9200-cm<sup>-1</sup> region.

In our temperature-dependent spectra we resolve a weak hump showing up at about 15 K sample temperature approximately 45 cm<sup>-1</sup> higher in energy than ZP2. This feature is smeared out significantly, probably due to a short lifetime. If we ascribe this hump to the transition  $\Gamma_4(^5E) \rightarrow \Gamma_3(^5T_2)$ , the  $\Gamma_3(^5T_2)$  state would be located some 40 cm<sup>-1</sup> above the lowest state of the  $^5T_2$  manifold, and could account for the steeper increase of the ZP1 and ZP2 linewidth at  $T > 10$  K (Fig. 3). At the present state of our knowledge, this assignment is only tentative, since this hump is very weak and obscured by instabilities in the spectral characteristics of our FTIR spectrometer showing up in this energy range. Crystal-field calculations<sup>1</sup> locate the  $\Gamma_3(^5T_2)$  state above the  $\Gamma_4(^5T_2)$ , as depicted in the left-hand part of Fig. 1. In contrast to these calculations our results hint to a change in the order of the  $\Gamma_4(^5T_2)$  and  $\Gamma_3(^5T_2)$  states, as can occur in systems with Jahn-Teller coupling. According to calculations of Ham and Slack<sup>12</sup> (Fig. 2), for Jahn-Teller coupling to  $E$ -mode distortions with  $\hbar\omega_E$  ( $\approx 300$  cm<sup>-1</sup>) greater than  $\lambda$  ( $\approx 100$  cm<sup>-1</sup>) such an inversion of order is possible. Our results on GaP:Fe also hint at such an interchange of both levels.<sup>10</sup> Also the next higher state  $\Gamma_5(^5T_2)$  is lowered significantly.

In our series of spectra recorded at increasing sample temperatures we find a reduction of the strength of the vibronic sideband with growing temperature (see increasing scaling factors in Fig. 2). This feature may be linked to Jahn-Teller coupling effects of the  $^5T_2$  state.

### III. CHARGE TRANSFER TRANSITIONS FROM $\text{Fe}^{3+}$ TO $[\text{Fe}^{2+}, h]$

The existence of photoinduced charge-transfer processes from  $\text{Fe}^{3+}$  to  $[\text{Fe}^{2+} + \text{hole}]$  was recognized in photoelectron paramagnetic resonance<sup>13</sup> and photoconductivity measurements.<sup>14</sup> These transitions lead to threshold-type onsets in the absorption at 0.78 and 1.13 eV (Fig. 4). Later, fine structures in the threshold regions were detected by CAS.<sup>6</sup> In our studies we recorded spectra with FTIR absorption spectroscopy on thick samples (~3 mm), which reveal many more details due to improved signal-to-noise ratio. We will first consider the lower threshold in more detail. To allow for the presen-

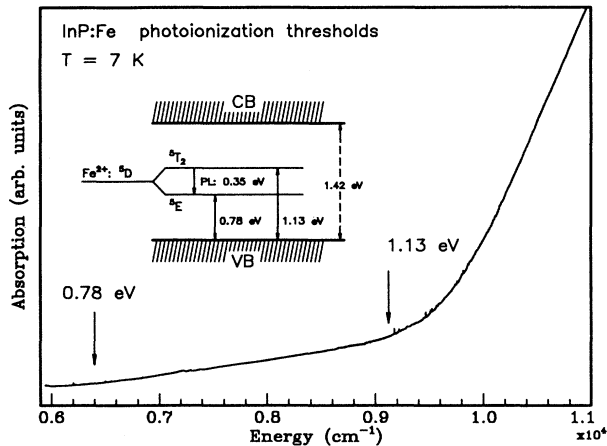


FIG. 4. Overview absorption spectrum of the two main photoionization thresholds observed for InP:Fe, corresponding to the transitions of electrons from the valence band into the  ${}^5E$  or  ${}^5T_2$  state of  $\text{Fe}^{2+}$ .

tation of even weak spectral features in more detail, we subtracted the broad background by fitting a polynomial of third degree to the region from 6200 to 7000  $\text{cm}^{-1}$ . The result is shown in Fig. 5.

The most prominent feature in this spectrum is a five-fold structure ( $X$ ) at  $\sim 6200 \text{ cm}^{-1}$ , which was ascribed to

excitation of an  $\text{Fe}^{3+}$ -bound exciton complex.<sup>6</sup> From their less-resolved conventional absorption spectra Wymolek and Hennel<sup>7</sup> propose a  $[\text{Fe}^{2+}, h]$  complex, by arguing that an ionization energy of 0.6 eV is too large for an exciton. The characteristic five-line pattern is repeated several times at higher energy due to coupling to  $\text{Fe}^{2+}$  defect-specific phonons. We observe mainly coupling to a gap mode GM1 with a vibrational energy of  $295 \text{ cm}^{-1}$ , and a local mode LM1 with an energy of  $349 \text{ cm}^{-1}$ . The frequency of GM1 is exactly the same as that observed in the Stokes phonon sideband in PL spectra of the  $\Gamma_5({}^5T_2) \rightarrow {}^5E$  transitions—that means a transition where a phonon is generated with the  $\text{Fe}^{2+}$  ion being in the  ${}^5E$  ground state.<sup>8,5</sup> If the  $\text{Fe}^{2+}$  ion is in the excited  ${}^5T_2$  state, the frequency of the normal mode GM1 is slightly shifted to  $292 \text{ cm}^{-1}$  ( $\equiv \text{GM1}^*$ ), as observed in absorption experiments on the internal  $3d$  transitions (Fig. 2). Since the change in electronic state of the  $\text{Fe}^{2+}$  ion from  ${}^5E$  to  ${}^5T_2$  already makes a significant change to the frequency of the GM1 phonon, we would expect it to be shifted much more for iron in charge states other than  $2+$ .

The other mode that couples to the fivefold absorption structure  $X$  at  $6200 \text{ cm}^{-1}$  has an energy of  $349 \text{ cm}^{-1}$  and is thus slightly lower in energy than the local mode LM1 ( $350 \text{ cm}^{-1}$ ) detected in the PL phonon sideband. The deviation is small, but clearly beyond experimental uncertainties of  $0.5 \text{ cm}^{-1}$ , and is identical to the transition related to  $\text{Fe}^{2+}$  directly, which will be discussed below.

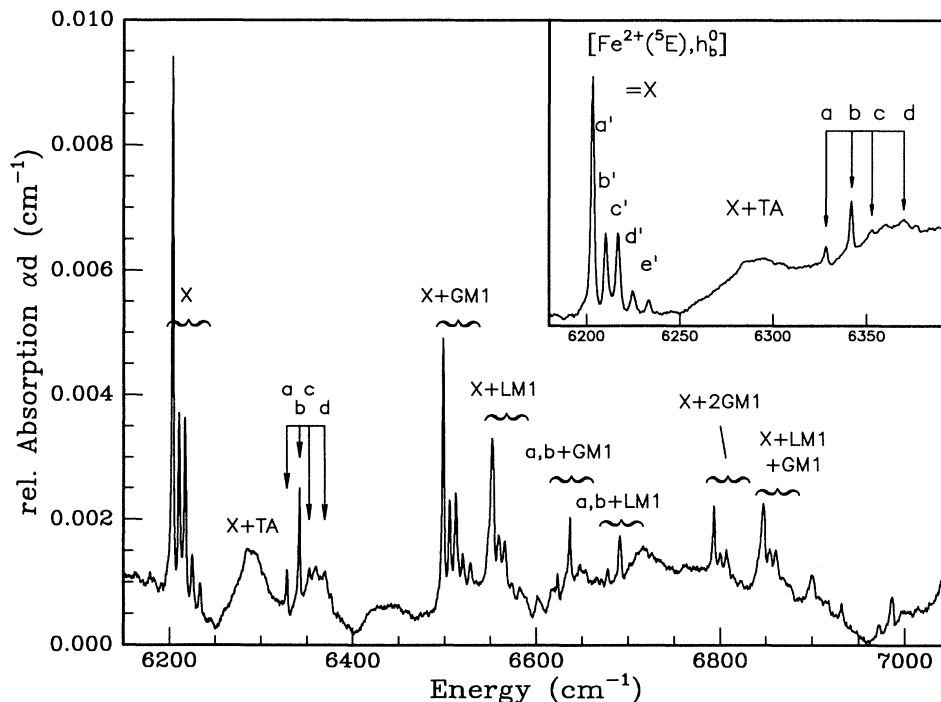


FIG. 5. Fine structure resolved at the onset of the first ionization threshold [process  $\text{Fe}^{3+} \rightarrow \text{Fe}^{2+} ({}^5E) + \text{hole}$ ]. Since all these weak absorptions are superimposed on a curved background, we subtracted for presentation purposes this background by fitting a polynomial of third degree. The most prominent feature resolved is the five-line structure  $X$ , which is ascribed to the generation of the complex  $[\text{Fe}^{2+} ({}^5E) + \text{shallow bound hole in its ground state}]$ . The transitions denoted by  $a-d$  are ascribed to processes, where the bound hole is left in its first excited state. For both features multiple phonon replicas caused by coupling to a  $\text{Fe}^{2+} ({}^5E)$ -specific gap mode (GM1) or local mode (LM1) are observed. The inset shows both electronic no-phonon transitions in an enlarged scale without subtraction of the background.

Since the energy of the two major phonon replicas of the  $X$  transitions is identical (GM1) or almost identical (LM1) in frequency to the phonons found for isolated  $\text{Fe}^{2+}$  in the  ${}^5E$  ground state, we conclude, that  $X$  must involve  $\text{Fe}^{2+}$  ( ${}^5E$ ) and not  $\text{Fe}^{3+}$ , as was proposed earlier.<sup>6</sup> The minor change in the  $350\text{-cm}^{-1}$  vibrational mode could be due to a slight change of the bonding forces by the influence of a bound hole (see below). The spectrum depicted in Fig. 5 was observed with lower resolution in magnetic circular dichroism studies<sup>15</sup> also. The (unresolved)  $X$  structure was also ascribed to the CT process  $\text{Fe}^{3+} \rightarrow [\text{Fe}^{2+}, h]$ , but the phonon replicas  $X + \text{GM1}$  and  $X + \text{LM1}$  were erroneously assigned to an independent transition  $\text{Fe}^{3+} \rightarrow \text{Fe}^{2+}$  ( ${}^5E$ ). The weaker structures  $a-d$  and their phonon replicas remained unresolved.

The assignment of  $X$  to an  $\text{Fe}^{2+}$ -related level is strongly supported by arguments obtained by a careful analysis of the spacing of the four ZP lines of the  ${}^5T_2 \rightarrow {}^5E$  internal transitions and the spacing of the five-line structure. The spacing of the  ${}^5E$  state and thus the spacing of the four ZP lines with the  $\Gamma_5({}^5T_2)$  as the final state in absorption is, within second-order perturbation theory, proportional to the square of the spin-orbit coupling parameter  $\lambda$  (Ref. 1) (Fig. 1). Figure 6 shows a comparison of the relative spacings of the four ZP lines (plus the calculated position of the  $\Gamma_2$  level) to the relative spacings of the peaks of the five-line structure  $X$ . For all three host materials InP, GaP, and GaAs, the splitting of the ZP lines is about the same. The splitting of the  $X$  subcomponents is approximately 0.5 times the ZP line splitting for all materials. This scaling law hints at a reduction of the spin-orbit coupling parameter  $\lambda$  by a factor of  $\approx 0.7$ , re-

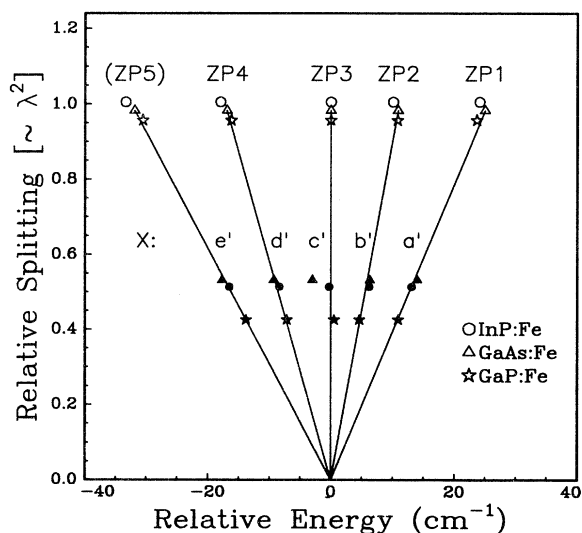


FIG. 6. Comparison of the splitting of the  $\text{Fe}^{2+}$   ${}^5E$  ground state (as measured on the four zero phonon transitions ZP1–ZP4) to the splitting of the  $X$  five-line structure. The position of the ZP5 forbidden transition is calculated theoretically from fitted values for  $Dq$  and  $\lambda$ . The positions of lines are aligned along the center component. For InP:Fe and GaP:Fe a scaling law with factors of 0.51 and 0.45 is valid. In the GaAs case this factor is 0.54, but the central component is shifted (Ref. 16).

sulting in a decrease of splittings by  $\approx (0.7)^2 \approx 0.5$ . This decrease must be caused by the influence of a bound hole on the  $\text{Fe}^{2+}$   $3d$  electrons, e.g., by spin-spin interaction. For the special case of InP:Fe we observe a reduction of the splittings to 51%, indicating a spin-orbit coupling parameter  $\lambda$  reduced to  $\sqrt{0.51} = 71\%$  of its previous value. For the system GaP:Fe, we observe a reduction of the splitting to 42%, and for GaAs:Fe to 53%. Characteristic deviations from the scaling for the center component of the GaAs  $X$  structure will be discussed in a forthcoming paper.<sup>16</sup> Since the scaling of splittings is not exactly proportional to  $\lambda^2$ , we took the values of  $\lambda$  reduced for InP by  $\sqrt{0.51}$ , and for GaAs by  $\sqrt{0.53}$ , and solved the crystal-field Hamiltonian

$$\mathcal{H}_{\text{CF}} = \frac{10}{120} Dq (O_4^0 + 5O_4^4) + \lambda \cdot \mathbf{L} \cdot \mathbf{S} \quad (4)$$

numerically for these reduced spin-orbit couplings. The resulting  ${}^5E$  splittings match within experimental error the line positions derived by the simple scaling law  $\sim \lambda^2$  used in Fig. 6.

In the spectrum of Fig. 5, we observe  $\sim 120\text{ cm}^{-1}$  above the  $X$  structure four additional peaks indicated by a set of arrows. The peaks  $a$  and  $b$  were also detected in previous studies.<sup>6–8</sup> The four peaks show exactly the same spacing as the four characteristic  $\text{Fe}^{2+}$  internal transition lines ZP1 to ZP4. The peaks  $a$  and  $b$  are separated by  $13.7\text{ cm}^{-1}$ , which is precisely the distance between ZP1 and ZP2. These peaks  $a$  and  $b$  couple again to the vibrational modes GM1 ( $295\text{ cm}^{-1}$ ), and LM1 ( $348.8\text{ cm}^{-1}$ ), which were found as replicas for the  $X$  pattern, and which are characteristic of the  $\text{Fe}^{2+}$   ${}^5E$  state. This indicates the close relationship of both transition series.

The interpretation of the  $X$  and  $a-d$  lines is summarized in Fig. 7. As proposed already by Juhl *et al.*,<sup>6</sup> the  $a-d$  lines are ascribed to charge-transfer transitions from  $\text{Fe}^{3+}$  to a complex consisting of  $\text{Fe}^{2+}$  plus a hole. But we discard the idea of generation of *free* holes, since this would result in spectral features like superimposed onsets of ionization thresholds, and not in sharp lines. We ascribe instead these transitions to processes, where *bound* holes are generated. If the bound hole is generated in its  $1s$ -like ground state, it has a significant overlap with the  $3d$  electrons. These are the  $X$  transitions. Already generation of the bound hole in the next excited state reduces this hole– $3d$ -electron interaction so far that within experimental error the undisturbed spacing of  ${}^5E$  levels is observed. These are the  $a-d$  transitions. Transitions to higher excited states of the hole vanish in the background absorption.

Corresponding charge-transfer transitions exist from  $\text{Fe}^{3+}$  to the excited  ${}^5T_2$  state of  $\text{Fe}^{2+}$  plus a bound hole. These show up in the energy range from  $9100$ – $10200\text{ cm}^{-1}$  and were in part already observed before.<sup>6–8</sup> Superimposed on a broad threshold of the CT process  $\text{Fe}^{3+} \rightarrow [\text{Fe}^{2+} + \text{free hole}]$ ,<sup>14</sup> multiple series of lines show up [Figs. 4 and 8(a)]. To show these lines in more clarity on an expanded scale, we have again subtracted the underlying broad ionization band by fitting a spline function [Fig. 8(b)]. Since our new spectra reveal many more de-

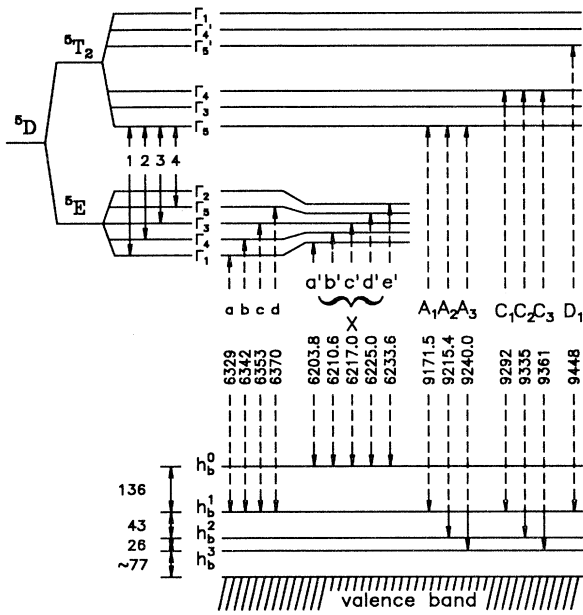


FIG. 7. Level scheme combining the experimental data on internal transitions  $\text{Fe}^{2+}$  and charge transfer transitions  $\text{Fe}^{2+} \rightarrow [\text{Fe}^{3+}, h]$ . Numbers give energies of the transitions in  $\text{cm}^{-1}$ .  $a'-e'$  denote the five subcomponents of the  $X$  structure.

tails than the spectra published hitherto, we have to alter several of the previous assignments. The identification of lines is mostly based on the perfect matching of energetic spacings of the different transitions.

The first series of lines, denoted by  $A_1, A_2, A_3$  in Fig. 8(b), starts at  $9171.5 \text{ cm}^{-1}$ , which is (within experimental uncertainty) the sum of the energies of the internal transition ZP1 plus the charge-transfer transition  $a$ . So, the  $A_1$  CT transition must leave the  $\text{Fe}^{2+}$  ion in the lowest state  $\Gamma_5$  out of the  ${}^5T_2$  manifold. The energy of  $292 \text{ cm}^{-1}$  of the phonon replicas  $A_1 + \text{GM1}^*$  (and for all other lines in this spectral region) is exactly that, which was found for these Fe-specific mode-in-absorption measurements on the ZP1 to ZP4 internal  $3d$  transitions.<sup>5</sup> This is an independent proof, that in all these transitions the  $\text{Fe}^{2+} {}^5T_2$  state must be involved. A second series of lines, now labeled  $C_1, C_2,$  and  $C_3$ , starts at  $9292 \text{ cm}^{-1}$ , i.e., shifted by  $119 \text{ cm}^{-1}$  relative to the  $A$  series. The energy of  $C_1$  is the sum of  $b + 2(\Gamma_4)$  (see Fig. 7).

The spacing of the subcomponents of the series ( $A_1, A_2, A_3$ ) and ( $C_1, C_2, C_3$ ) are identical. We ascribe each of these series to processes ending in a sequence of excited states of the bound hole. The lines increase in their half-width within each series, and from the  $A_i - C_i$  series: the FWHM of  $A_1$  is  $\cong 2.2 \text{ cm}^{-1}$ ,  $A_2$  has  $5 \text{ cm}^{-1}$ , and  $C_1$  already has  $13 \text{ cm}^{-1}$ . Since the lines are Lorentzian in their line shape (except line  $A_1$ , which is Gaussian), the increasing half-width is due to the shorter lifetime of the final states: excited-hole states can relax quickly to the hole ground state, and the electron generated in the  $\text{Fe}^{2+} \Gamma_4({}^5T_2)$  state can relax quickly into the  $\Gamma_5({}^5T_2)$  state. The short lifetime of the excited hole contributes

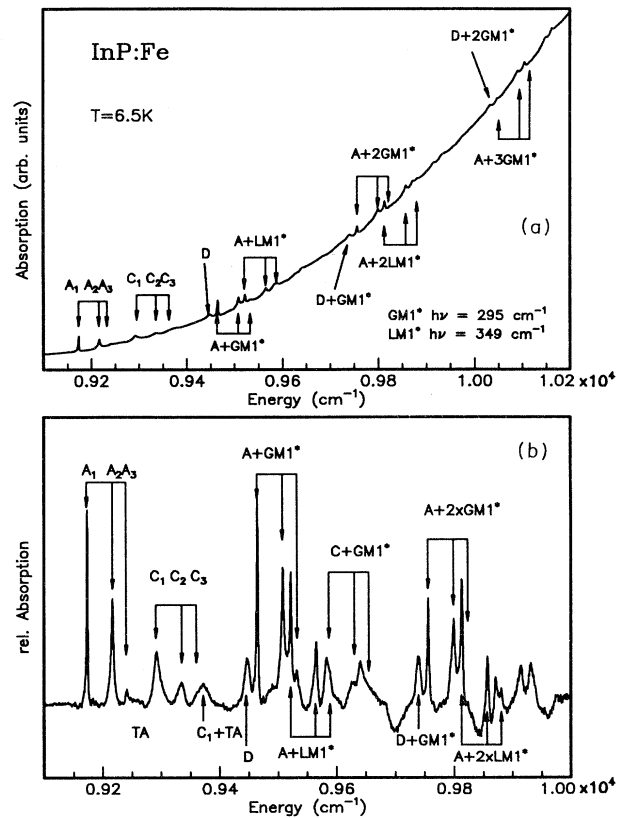


FIG. 8. (a) Fine structure of the second photoionization threshold  $\text{Fe}^{3+} \rightarrow [\text{Fe}^{2+}({}^5T_2) + h]$ . Superimposed on a curved background are several features, which are shown in more detail in part (b) of this picture. The background was subtracted by fitting a spline curve. The main features are absorptions due to CT processes ending in the lowest  $\text{Fe}^{2+} {}^5T_2$  state  $\Gamma_5$ , and generation of a hole in series of excited states (lines  $A_1 - A_3$ ). The  $C_1 - C_3$  series of lines is introduced by the analogous process ending in the  $\text{Fe}^{2+} \Gamma_4({}^5T_2)$  state (see also Fig. 7). Line  $D$  is ascribed to the transition into  $\text{Fe}^{2+} \Gamma_5'({}^5T_2)$ . All other features are phonon replicas of these purely electronic transitions, induced by coupling to phonons specific for  $\text{Fe}^{2+}$  in its  ${}^5T_2$  state.

significantly to the broadening of transition  $C_1$ , since the  $\text{Fe}^{2+}$  internal transition  $2(\Gamma_4)$  ending on the same  $\Gamma_4({}^5T_2)$  level has only a FWHM of  $\cong 6 \text{ cm}^{-1}$ , i.e., about half the FWHM of  $C_1$ .

One more CT transition, which we consider as purely electronic in nature, is observed at  $9446 \text{ cm}^{-1}$  [labeled  $D$  in Fig. 8(b)]. This transition generates a hole in the first excited bound state  $h_b^1$  and an electron in the  $\Gamma_5({}^5T_2)$  state. All other resonances observed in the spectrum of Fig. 8(b) are phonon replicas of the zero phonon CT transitions mentioned so far. A possible transition  $B_1$  generating  $\text{Fe}^{2+}$  ions in the  $\Gamma_3({}^5T_2)$  state would accidentally coincide with the  $A_2$  line and remains thus invisible, perhaps leaving its traces in the slight asymmetry of  $A_2$ .

There remains the question of why we do not see a transition analogous to  $X$ , i.e., a CT process, where a

bound hole is generated in the ground state. If such a process occurred, again one would have to expect an influence of the hole on the spin-orbit coupling parameter  $\lambda$  of the Fe  $3d$  electrons now in the  ${}^5T_2$  state, lowering  $\lambda$  presumably again to  $\approx 70\%$  of its original value. This would mean for the  $\Gamma_5({}^5T_2)$  state, which is approximately  $10 Dq + 3\lambda$  above the  ${}^5E$  state,<sup>1</sup> an increase in energy by about  $75 \text{ cm}^{-1}$ , since  $\lambda (\cong -90 \text{ cm}^{-1})$  is negative.<sup>5</sup> The  $\Gamma_4$  state should thus move up by  $\cong 25 \text{ cm}^{-1}$ . So a CT transition generating a bound hole in the ground state and an  $\text{Fe}^{2+}$  ion in its lowest  ${}^5T_2$  substate is energetically less favorable than processes leaving the hole in a first excited state. If transitions to this metastable state now exist, we expect them to be drastically broadened due to the very short lifetime expected for such a state, and the respective absorption peaks should vanish in the background absorption.

The coupling of all charge-transfer transitions to lattice and Fe-specific phonons is stronger than for the pure  $3d$  internal transitions. We ascribe this effect to the involvement of the shallow bound hole with its more extended wave function in this class of processes.

We take now a closer look at the binding energy of the shallow bound hole. If we assume that the reduction of  $\lambda$  within the  $\text{Fe}^{2+}$  ( ${}^5E$ ) state leaves the center of gravity for these states unaffected,<sup>17</sup> the spacing of the  $h_b^0$  state from the first excited  $h_b^1$  state can be evaluated from energy difference of the transitions  $c$  and  $c'$  (Fig. 7):

$$\begin{aligned} E(h_b^1) - E(h_b^0) &= E(c) - E(c') \\ &= 6353 - 6217 = 136 \text{ cm}^{-1}. \end{aligned} \quad (5)$$

The energy differences to the next excited states can be directly evaluated from the distances of lines  $A_1$ ,  $A_2$ , and  $A_3$ . Figure 9 compares these energies to those of the common acceptors carbon and zinc in InP, and to effective-mass theory values.<sup>18,19</sup> It seems reasonable to identify the excited-hole states  $h_b^1$ ,  $h_b^2$ , and  $h_b^3$  with the  $2P_{3/2}$ ,  $2P_{5/2}$  ( $\Gamma_8$ ), and  $2P_{5/2}$  ( $\Gamma_7$ ) states, respectively, since their spacings are comparable to those of the acceptors cited as reference in Fig. 9. If we align these  $\text{Fe}^{2+}$   $2P$  acceptor states on the energy scale with the other acceptors, we end up with an ionization energy of  $282 \pm 10 \text{ cm}^{-1}$  for the ground state of the hole bound to  $\text{Fe}^{2+}$ . This is somewhat less than the value predicted by effective-mass theory (EMT), and indicates that the central core potential of  $\text{Fe}^{2+}$  ions is slightly repulsive for holes.

If this interpretation of our spectra and assignment to bound-hole states holds, very precise energies for the location of the  $\text{Fe}^{2+}/\text{Fe}^{3+}$  levels in the band gap can be quoted: the lowest  ${}^5E$  state is found  $6475 \pm 10 \text{ cm}^{-1}$  ( $= 802.8 \pm 1.2 \text{ meV}$ ) above the valence-band edge (at  $4.2 \text{ K}$ ), and the lowest  ${}^5T_2$  state  $\Gamma_5$  is at  $9318 \pm 10 \text{ cm}^{-1}$  ( $= 1155.3 \pm 1.2 \text{ meV}$ ).

Evidence for the existence of a bound-hole state for  $\text{Fe}^{2+}$  ions comes also from time-resolved PL measurements. Klein, Furneaux, and Henry<sup>20</sup> explain the occurrence of a minimum for the temperature dependence of the electron capture coefficient for  $\text{Fe}^{2+}$  ions around

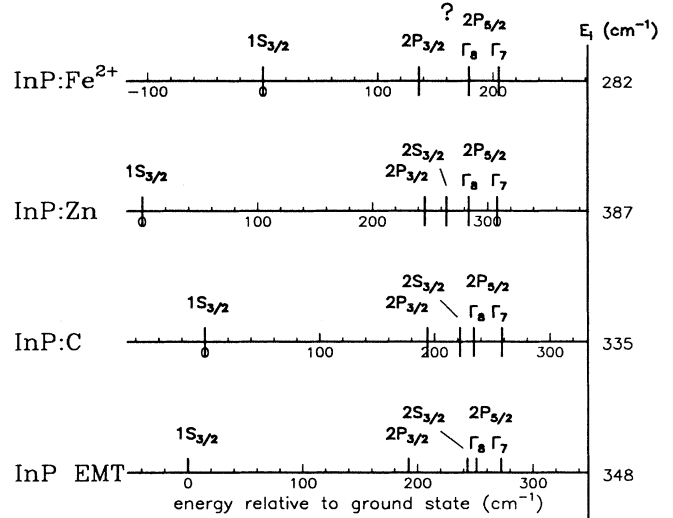


FIG. 9. Comparison of the  $\text{Fe}^{2+}$  bound hole localization energies to those of common acceptors and effective-mass theory values. The latter energies were taken from Ref. 19. The energy scales of the reference acceptors are aligned with respect to their ionization energies  $E_i$ . The  $\text{Fe}^{2+}$  bound-hole energies are shifted such that the excited states, which are tentatively ascribed to various  $2P$  acceptor levels, match those of the other acceptors. From this arrangement we derive a  $\text{Fe}^{2+}$  hole binding energy of  $282 \pm 10 \text{ cm}^{-1}$  ( $35 \pm 1.5 \text{ meV}$ ).

$50 \text{ K}$  (see Fig. 5 in Ref. 20) with the existence of a  $\text{Fe}^{3+}$  bound state for electrons. A similar minimum is observed in the temperature dependence of the hole capture at  $\text{Fe}^{2+}$  (Ref. 20, Fig. 8), but not discussed any further. In view of our results, we believe that as an analog to ( $\text{Fe}^{3+}, e$ ) a state ( $\text{Fe}^{2+}, h$ ) is responsible for this effect.

The model discussed here for the charge-transfer transitions in  $\text{InP:Fe}$  also consistently explains the analogous spectra observed for  $\text{GaAs:Fe}$  (Refs. 7, 10, and 11) and  $\text{GaP:Fe}$ .<sup>10,21</sup> It removes the discrepancy between the ionization threshold as determined by a fit to the onset of the broad absorption band<sup>21</sup> and the binding energies of holes as quoted before, where the  $a$  CT transition was considered to end in the hole ground state instead of the first excited state.

#### IV. CONCLUSIONS

We performed a detailed study of the Fe-related transitions in  $\text{InP}$  by FTIR absorption spectroscopy. Temperature-dependent spectra allow us to deduce the level scheme for the internal  $3d$  transitions of  $\text{Fe}^{2+}$  in  $\text{InP}$ . Absorptions in the energy ranges around  $6200$  and  $9200 \text{ cm}^{-1}$  are interpreted as charge-transfer transitions from  $\text{Fe}^{3+}$  to  $\text{Fe}^{2+}$  plus bound hole states. In the ground state the hole strongly influences the  $\text{Fe}^{2+}$   $3d$  electrons, reducing their spin-orbit coupling, thus giving rise to a characteristic fivefold structure at about  $6170 \text{ cm}^{-1}$ . Additional structures are interpreted as transitions to excited bound hole states. By comparison of these excited

hole states to those of common shallow acceptors and EMT predictions, a hole binding energy of  $282 \pm 10 \text{ cm}^{-1}$  is derived for  $\text{Fe}^{2+}$ . With the same accuracy the  $\text{Fe}^{2+}$   ${}^5E$  and  ${}^5T_2$  levels can be located in the bandgap. The model presented here consistently explains all the features observed in the PL and absorption spectra.

#### ACKNOWLEDGMENTS

We thank A. Dörnen for valuable discussions. The financial support of the Deutsche Forschungsgemeinschaft (DFG), Bonn, Germany, under Contract No. TH-419 is gratefully acknowledged.

- 
- <sup>1</sup>W. Low and M. Weger, Phys. Rev. **118**, 1119 (1960).  
<sup>2</sup>G. A. Slack, S. Roberts, and F. S. Ham, Phys. Rev. **155**, 170 (1966).  
<sup>3</sup>W. H. Koschel, U. Kaufmann, and S. G. Bishop, Solid State Commun. **21**, 1069 (1977).  
<sup>4</sup>P. Leyral, C. Charreaux, and G. Guillot, J. Lumin. **40/41**, 329 (1988).  
<sup>5</sup>K. Pressel, K. Thonke, A. Dörnen, and G. Pensl, Phys. Rev. B **43**, 2239 (1991).  
<sup>6</sup>A. Juhl, A. Hoffmann, D. Bimberg, and H. J. Schulz, Appl. Phys. Lett. **50**, 1292 (1987).  
<sup>7</sup>A. Wymolek and A. M. Hennel, Acta Phys. Pol. A **77**, 67 (1990).  
<sup>8</sup>K. Pressel, K. Thonke, and A. Dörnen, in *Proceedings of the 20th International Conference on the Physics of Semiconductors, Thessalonika, Greece, 1990*, edited by E. M. Anastassakis and J. D. Joannopoulos (World Scientific, Singapore, 1990), p. 690.  
<sup>9</sup>The electric and magnetic dipole transitions within the  ${}^5E$  state cannot account for efficient thermalization, since their lifetime is on the order of hours, as has been found for  $\text{Fe}^{2+}$  in tetrahedral ZnS [G. A. Slack, S. Roberts, and F. S. Ham, Phys. Rev. **155**, 170 (1967)]. But also in ZnS the lifetime is determined by nonradiative processes, resulting in a FWHM of the lines on the order of  $5 \text{ cm}^{-1}$ .  
<sup>10</sup>G. Rückert *et al.* (unpublished).  
<sup>11</sup>K. Pressel, G. Rückert, K. Thonke, and A. Dörnen (unpublished).  
<sup>12</sup>F. S. Ham and G. A. Slack, Phys. Rev. B **4**, 777 (1971).  
<sup>13</sup>G. H. Stauss, J. J. Krebs, and R. L. Henry, Phys. Rev. B **16**, 974 (1977).  
<sup>14</sup>S. Fung, R. J. Nicholas, and R. A. Stradling, J. Phys. C **12**, 5145 (1979).  
<sup>15</sup>A. Görger, B. K. Meyer, and J. M. Spaeth, in *International Conference on Semi-Insulating III-V-Materials, Malmö, Sweden*, edited by G. Grossmann and L. Ledebø (North-Holland, Amsterdam, 1988), p. 331.  
<sup>16</sup>K. Pressel *et al.* (unpublished).  
<sup>17</sup>If the center of gravity for the whole  ${}^5D$  manifold is assumed to remain constant, the reduction of  $\lambda$  as quoted in the text leaves the uppermost  ${}^5E$  state  $\Gamma_2$  constant, but moves all other states proportionally up. Especially the middle state  $\Gamma_3$  is lifted by  $13.2 \text{ cm}^{-1}$ , as determined numerically from the Hamiltonian, Eq. (4). As a consequence, the energy difference between the two lowest bound-hole states would evaluate to  $E(h_b^1) - E(h_b^0) \approx 149 \text{ cm}^{-1}$  instead of  $136 \text{ cm}^{-1}$  as quoted in Eq. (5). Also, the ionization energy of  $[\text{Fe}^{2+}, h]$  changes to  $295 \text{ cm}^{-1}$ , instead of  $282 \text{ cm}^{-1}$  (Fig. 9).  
<sup>18</sup>A. Baldereschi and N. O. Lipari, Phys. Rev. B **9**, 1525 (1974).  
<sup>19</sup>P. J. Dean, D. J. Robbins, and S. G. Bishop, Solid State Commun. **32**, 379 (1979).  
<sup>20</sup>P. B. Klein, J. E. Furneaux, and R. L. Henry, Phys. Rev. B **29**, 1947 (1984).  
<sup>21</sup>T. Wolf, D. Bimberg, and W. Ulrici, Phys. Rev. B **43**, 10004 (1991).